Fracturation hydraulique et stimulation hydraulique

Francois Henri Cornet, Institut de Physique du Globe de Strasbourg

Principe de la fracturation hydraulique

Rôle du champ de contrainte sur la géométrie des grandes fractures hydrauliques

Stimulation hydraulique : l’exemple de Soultz/sous Forêts

Le question posée par l’exploitation des « gaz de shistes »

Hydraulic fracturing

- The stress field close to a cylindrical hole in an elastic field is :

$$\sigma_{\rho\rho} = \left[1-\frac{r^2}{\rho^2}\right]\frac{\sigma_{11}^{\infty}+\sigma_{22}^{\infty}}{2} + \left[1-\frac{4r^2}{\rho^2}+\frac{3r^4}{\rho^4}\right]\left[\frac{\sigma_{11}^{\infty}-\sigma_{22}^{\infty}}{2}\cos 2\theta + \sigma_{12}^{\infty}\sin 2\theta\right]$$

$$\sigma_{\theta\theta} = \left[1+\frac{r^2}{\rho^2}\right]\frac{\sigma_{11}^{\infty}+\sigma_{22}^{\infty}}{2} - \left[1+\frac{3r^2}{\rho^2}\right]\left[\frac{\sigma_{11}^{\infty}-\sigma_{22}^{\infty}}{2}\cos 2\theta + \sigma_{12}^{\infty}\sin 2\theta\right]$$

$$\sigma_{zz} = \sigma_{33}^{\infty} - 4\nu\frac{r^2}{\rho^2}\left[\frac{\sigma_{11}^{\infty}-\sigma_{22}^{\infty}}{2}\cos 2\theta + \sigma_{12}^{\infty}\sin 2\theta\right]$$

$$\sigma_{\theta z} = \left[1+\frac{r^2}{\rho^2}\right](\sigma_{23}^{\infty}\cos\theta - \sigma_{31}^{\infty}\sin\theta)\ ;\quad \sigma_{z\rho} = \left[1-\frac{r^2}{\rho^2}\right](\sigma_{31}^{\infty}\cos\theta + \sigma_{23}^{\infty}\sin\theta)$$

$$\sigma_{\theta\rho} = \left[1+\frac{2r^2}{\rho^2}-\frac{3r^4}{\rho^4}\right]\left[\frac{\sigma_{22}^{\infty}-\sigma_{11}^{\infty}}{2}\sin 2\theta + \sigma_{12}^{\infty}\cos 2\theta\right]$$

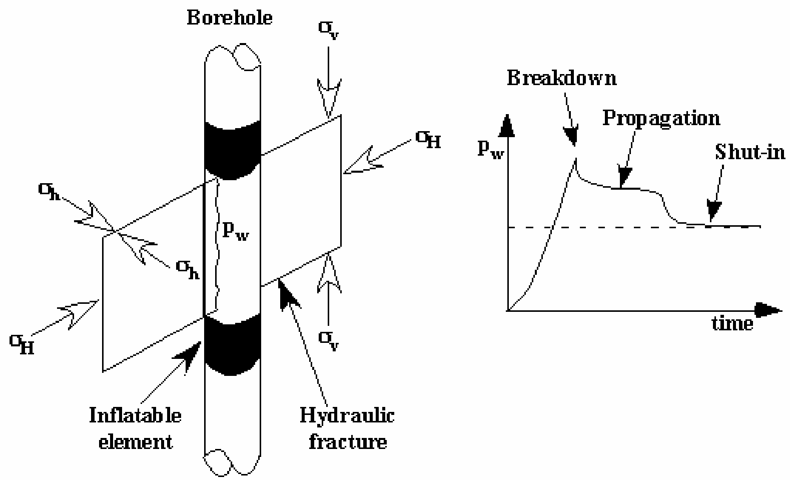

- If the borehole is parallel to a principal stress direction (Vertical) and a pressure is applied in the hole: $\sigma_{\theta\theta} = (\sigma_H + \sigma_h) - 2(\sigma_H - \sigma_h)\cos 2\theta - P_w$, and rupture occurs for :

$$\sigma_{\theta\theta} = -\sigma_H + 3\sigma_h - P_w + \sigma^T$$

- If the rock has been cooled down by mud circulation, the hoop stress is : $\sigma_{\theta\theta} = -K\Delta T/E$, where K is coefficient of thermal expansion, E is Young's modulus and ΔT is the difference between far-field and borehole temperature

- Correction for pore pressure effect (still debated)

- Both hydraulic fracturing and thermal cracking are mode I fractures

Generating en echelon fractures in inclined wells

$$\sigma_{\rho\rho} = \left(1-\frac{r^2}{\rho^2}\right)\frac{\sigma_{11}^{\infty}+\sigma_{22}^{\infty}}{2} + \left(1-\frac{4r^2}{\rho^2}+\frac{3r^4}{\rho^4}\right)\left(\frac{\sigma_{11}^{\infty}-\sigma_{22}^{\infty}}{2}\cos 2\theta + \sigma_{12}^{\infty}\sin 2\theta\right) \quad + P_w$$

$$\sigma_{\theta\theta} = \left(1+\frac{r^2}{\rho^2}\right)\frac{\sigma_{11}^{\infty}+\sigma_{22}^{\infty}}{2} - \left(1+\frac{3r^2}{\rho^2}\right)\left(\frac{\sigma_{11}^{\infty}-\sigma_{22}^{\infty}}{2}\cos 2\theta + \sigma_{12}^{\infty}\sin 2\theta\right) \quad - P_w$$

$$\sigma_{zz} = \sigma_{33}^{\infty} - 4\nu\frac{r^2}{\rho^2}\left(\frac{\sigma_{11}^{\infty}-\sigma_{22}^{\infty}}{2}\cos 2\theta + \sigma_{12}^{\infty}\sin 2\theta\right) \qquad (32)$$

$$\sigma_{\theta z} = \left(1+\frac{r^2}{\rho^2}\right)(\sigma_{23}^{\infty}\cos\theta - \sigma_{31}^{\infty}\sin\theta)\;;\quad \sigma_{z\rho} = \left(1-\frac{r^2}{\rho^2}\right)(\sigma_{31}^{\infty}\cos\theta + \sigma_{23}^{\infty}\sin\theta)$$

$$\sigma_{\theta\rho} = \left(1+\frac{2r^2}{\rho^2}-\frac{3r^4}{\rho^4}\right)\left(\frac{\sigma_{22}^{\infty}-\sigma_{11}^{\infty}}{2}\sin 2\theta + \sigma_{12}^{\infty}\cos 2\theta\right)$$

- effects on borehole failure

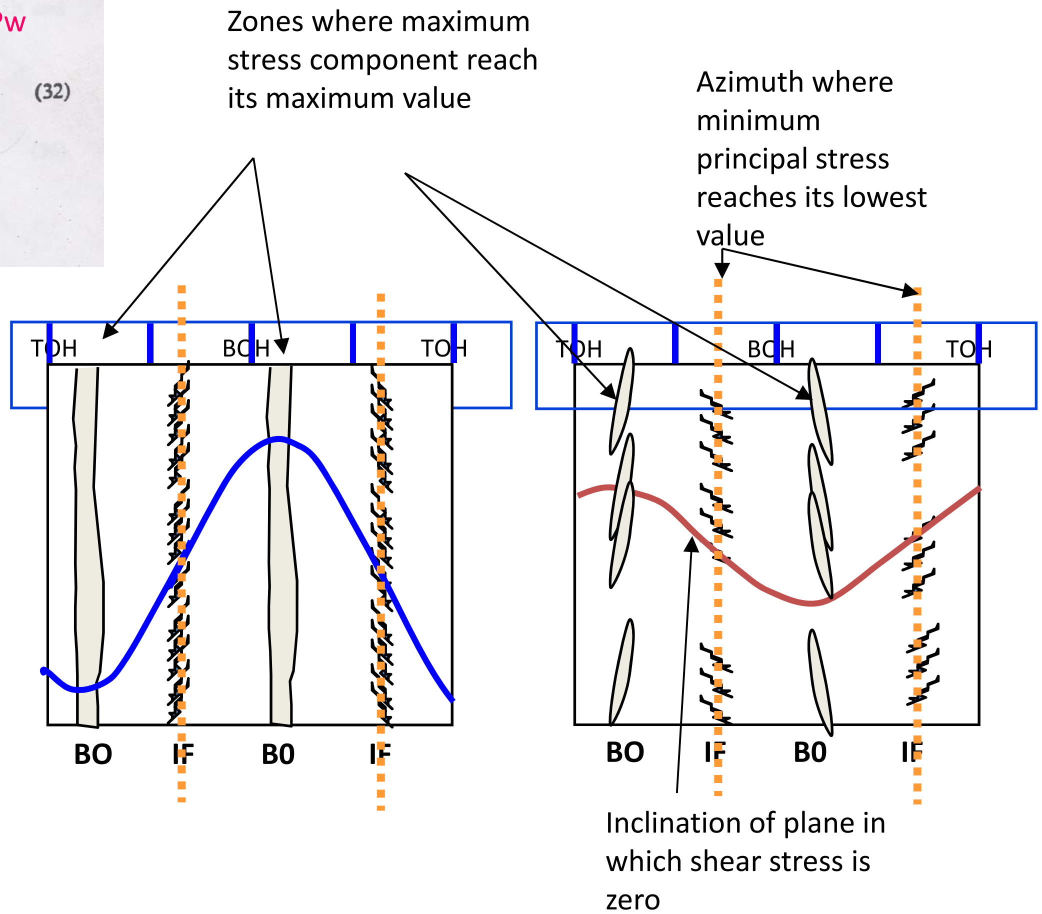

The case of horizontal wells

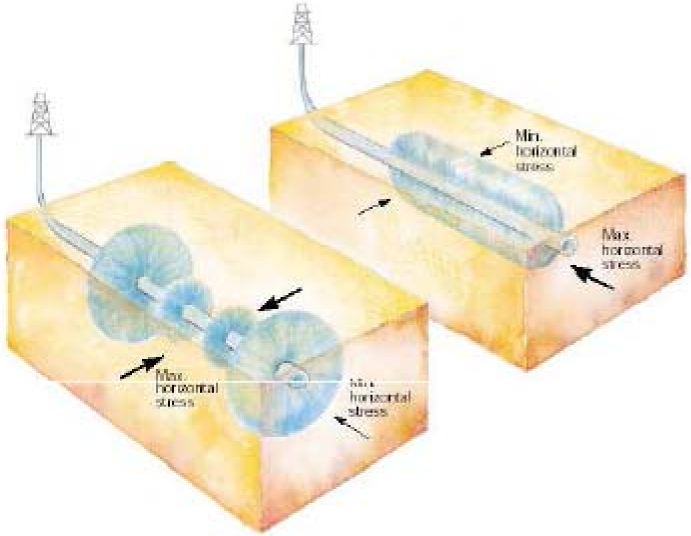

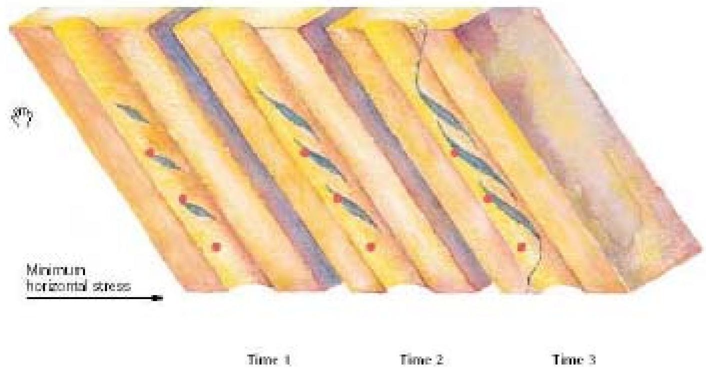

22 JD
091118

Field level

Schlumberger

Keeping the fracture open:
Propped fracture

- Fracture is kept open with proppant
  - sand: jordan
  - ceramic: ISP , Carbolite
  - bauxite
- With a particular distribution (Mesh Size)
  - Generally mesh 20/40 or 0.84 to 0.43 mm
- The thickness of the final proppant pack should be in the range of at least 3 layers of proppant
- Used for siliclastic reservoirs and in carbonates in some cases (chalk)

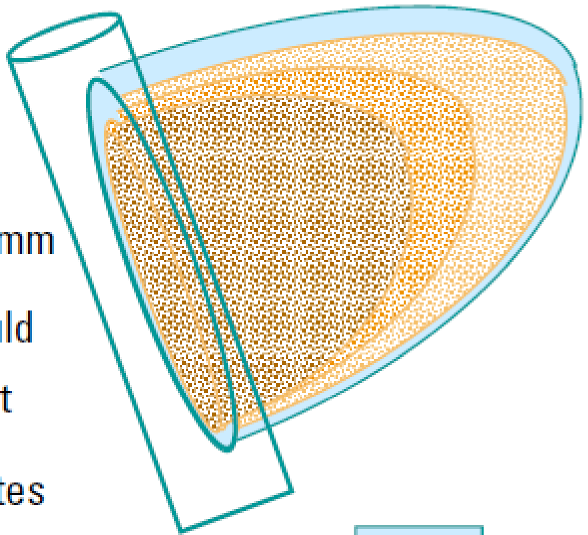

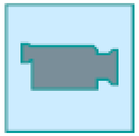

Schlumberger

De injection d'un agent de soutènement pour les vraies fractures hydrauliques

Keeping the fracture open:
Acid fracturing

- A high conductivity channel is created by dissolving part of the fractures face with acid.
- The fracture closes, and the path consists in channels created by the roughness of the fracture walls
  - Dissolution should not be uniform: any uniform dissolution will be closed by stress.
- For carbonate reservoirs only

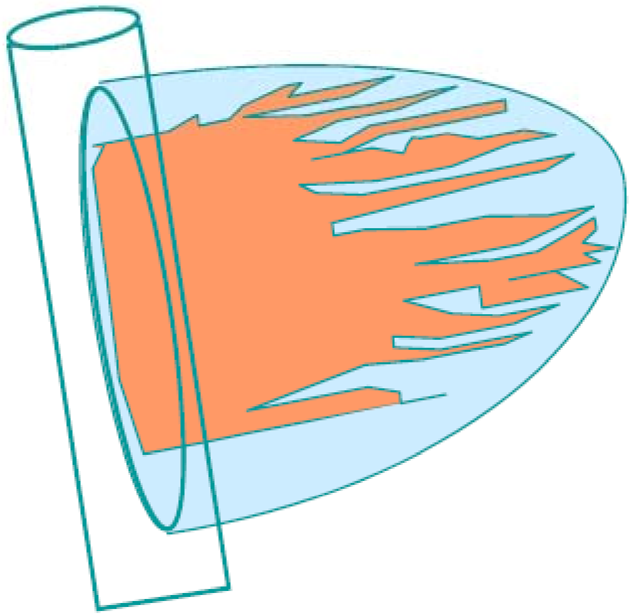

Influence de la contrainte principale minimum sur la géométrie des fractures

Fracturation hydraulique = Rupture de traction pure

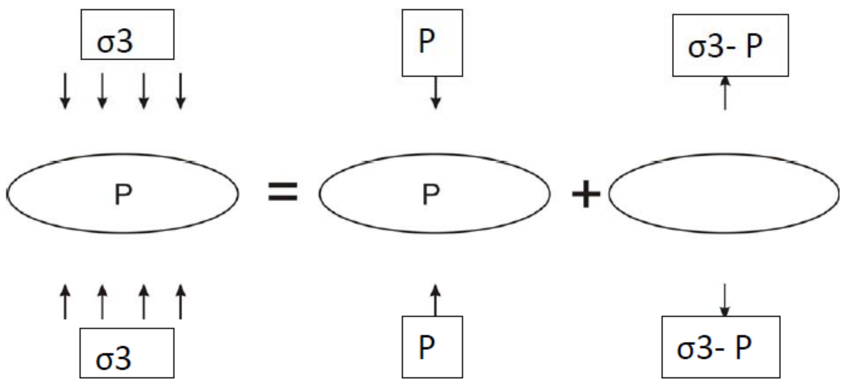

Facteur d'intensité de contrainte $K_I \alpha (\sigma_3\text{-}P)(2\pi\ l)^{1/2}$;
rupture si $K_I = K_{Ic}$

Extension spatiale des fractures hydrauliques en terrain homogène

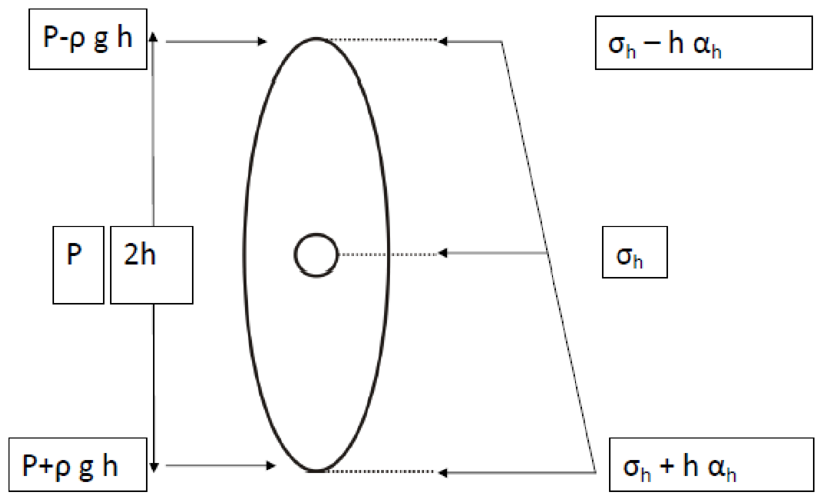

Cas des terrains sédimentaires (bassin de Paris)

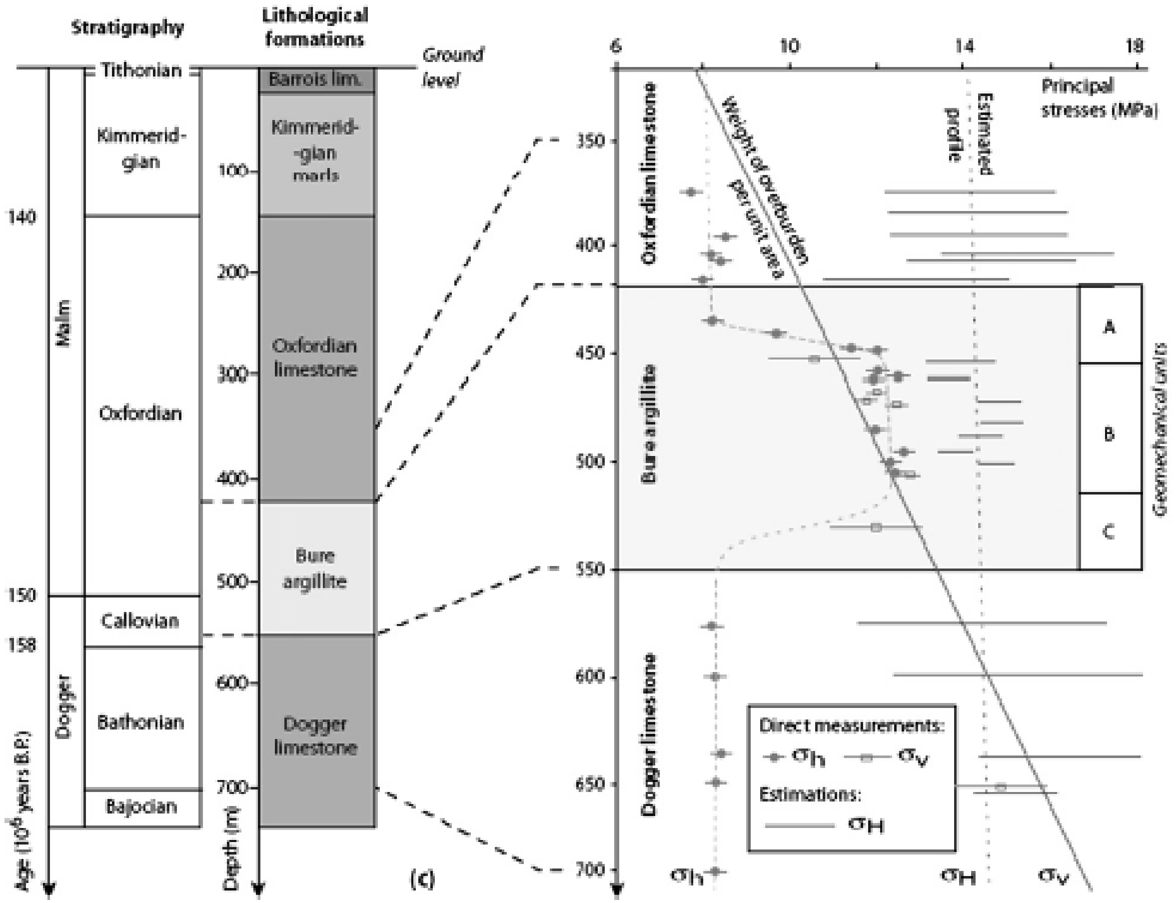

Stimulation hydraulique sur le site expérimental de Soultz/forêts

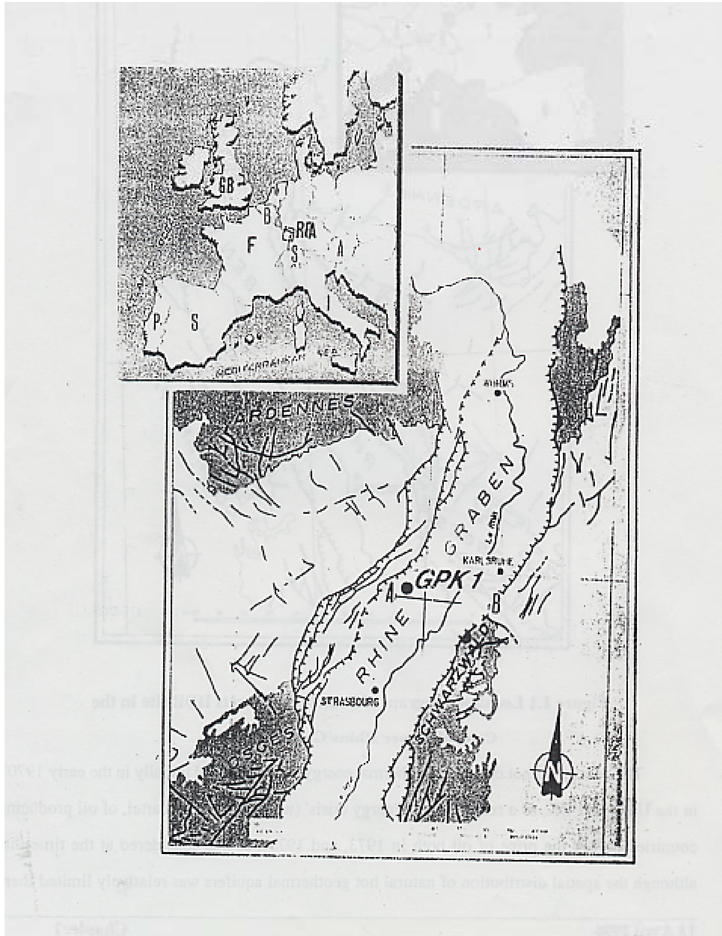

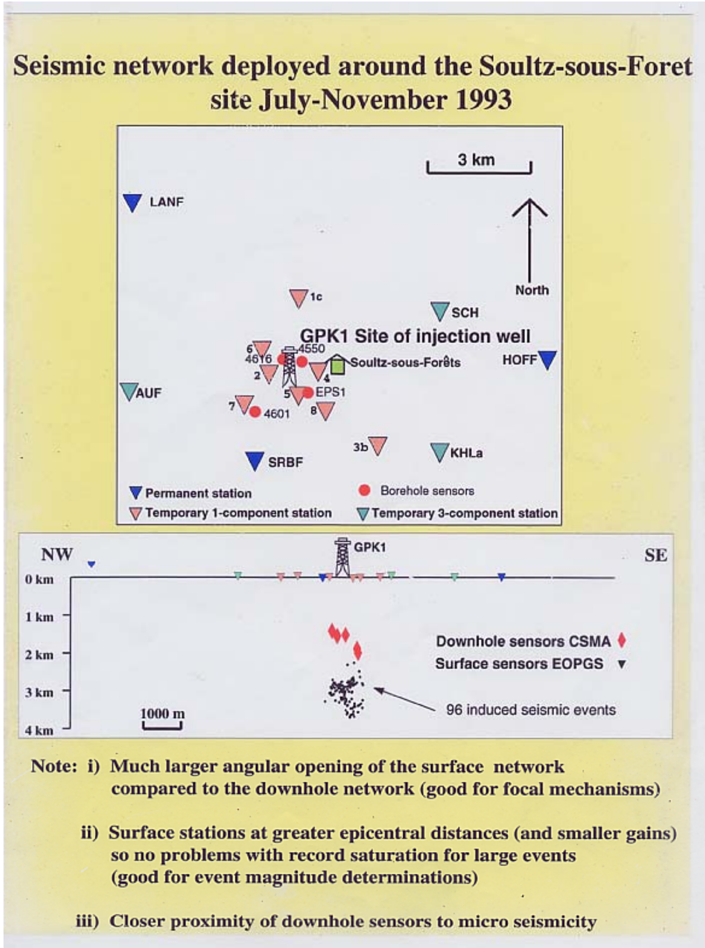

Objectif : induire des mouvements de cisaillement le long de fractures préexistantes. Résultats du premier essai de stimulation (2850-3400 m) (Sept. 1993)

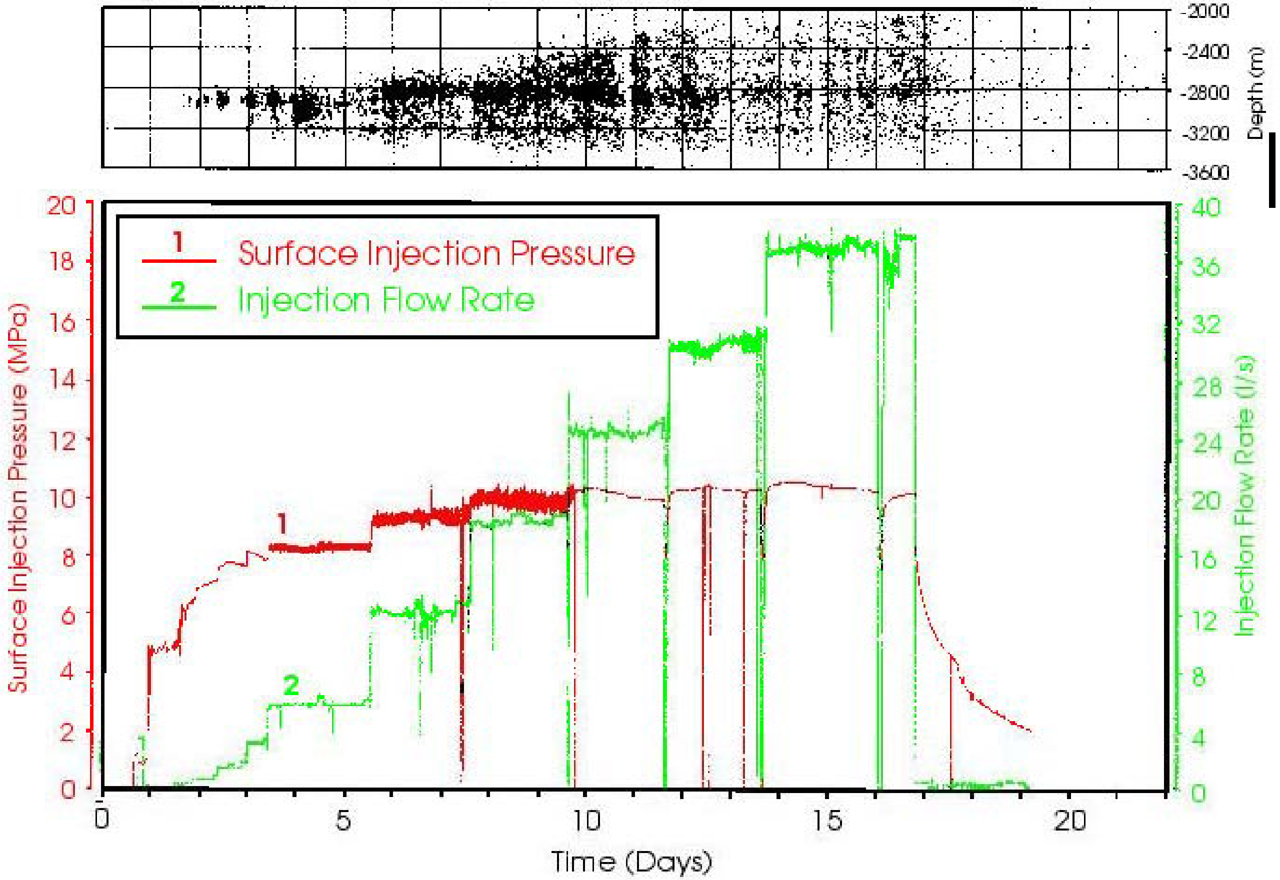

Localisation des événements microsismiques

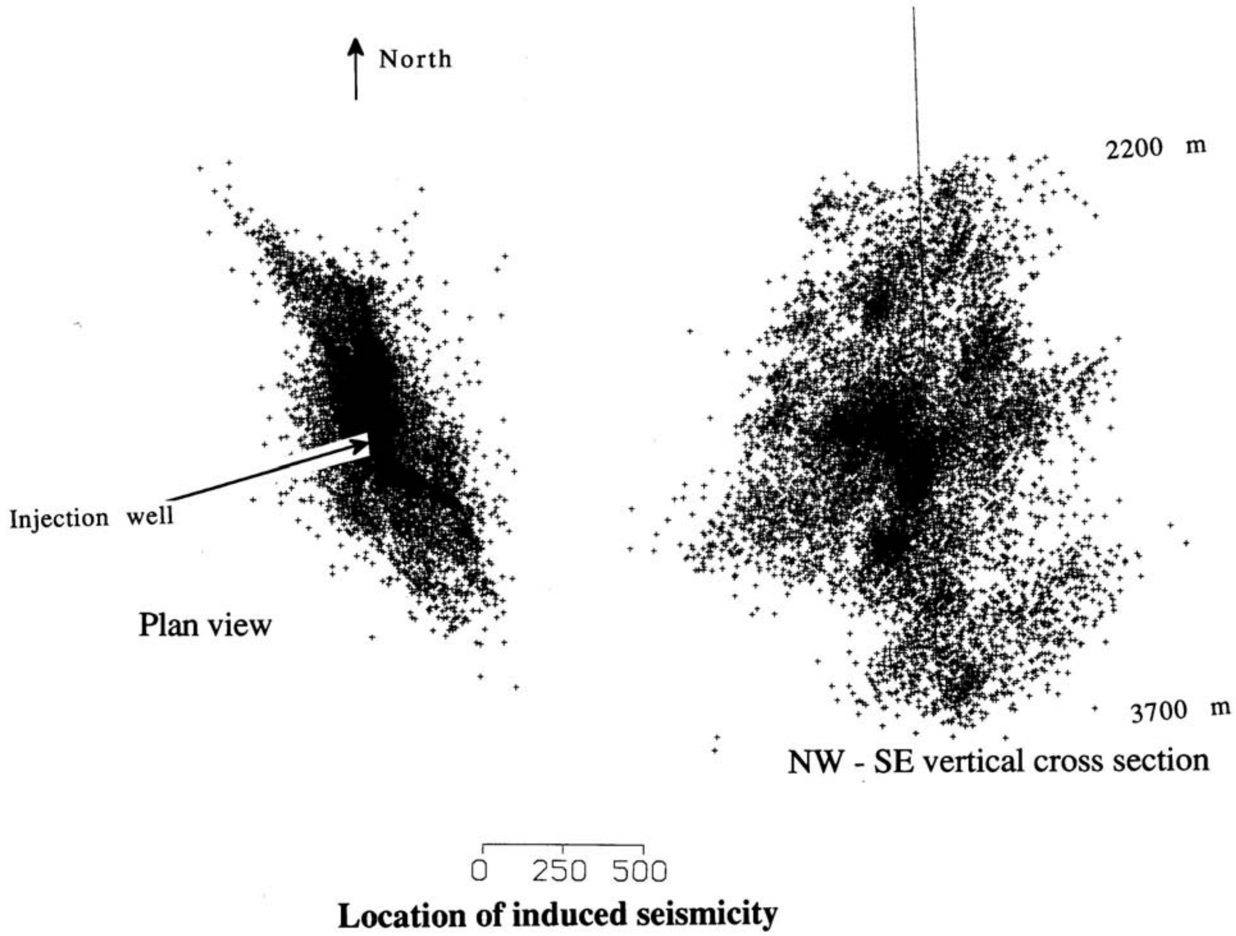

Etude à différentes profondeurs de l'orientation du nuage

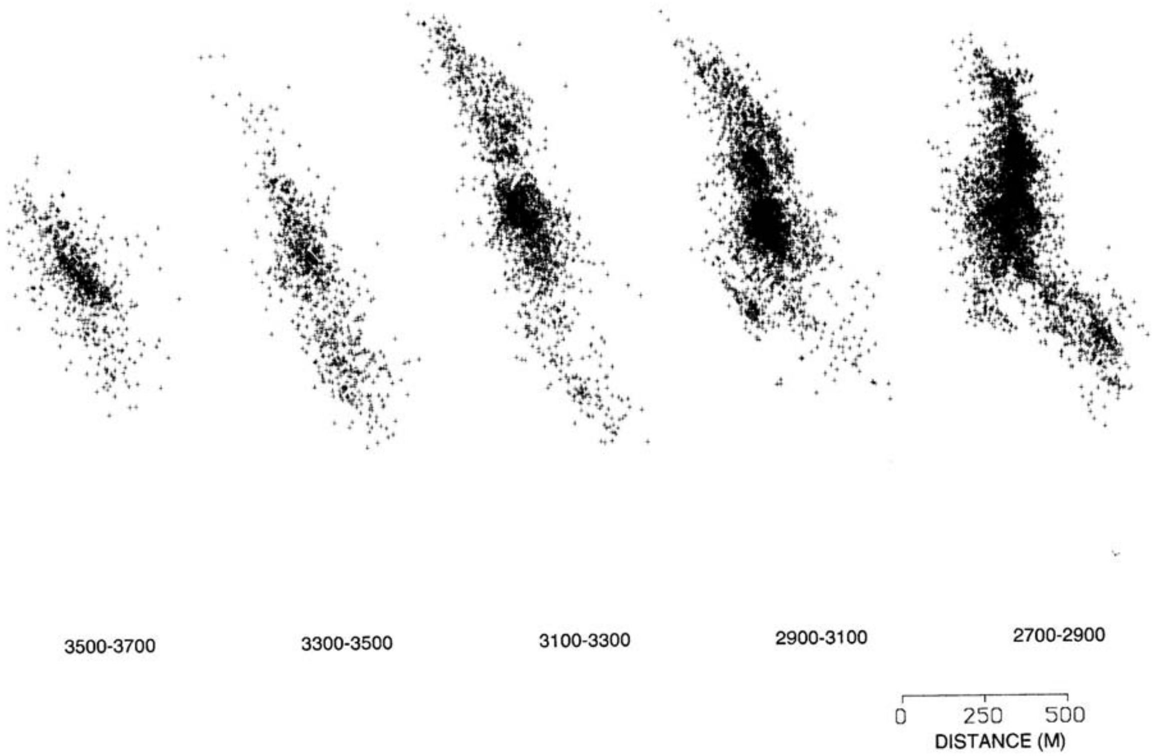

Détermination de l'orientation de la contrainte maximum horizontale à partir des ovalisations de forage et des ruptures thermiques

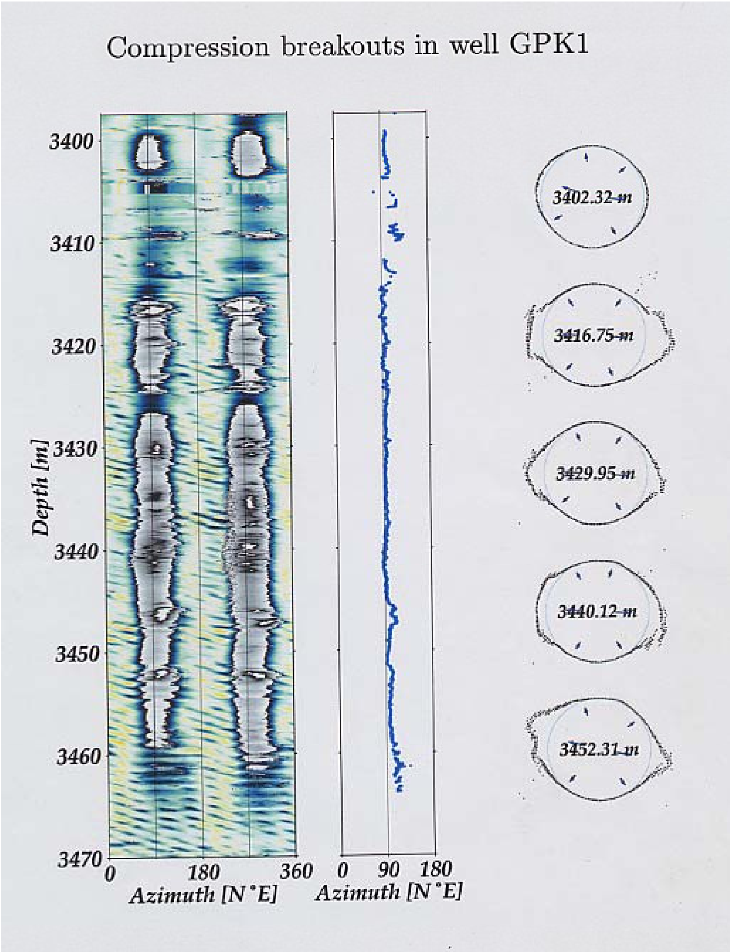

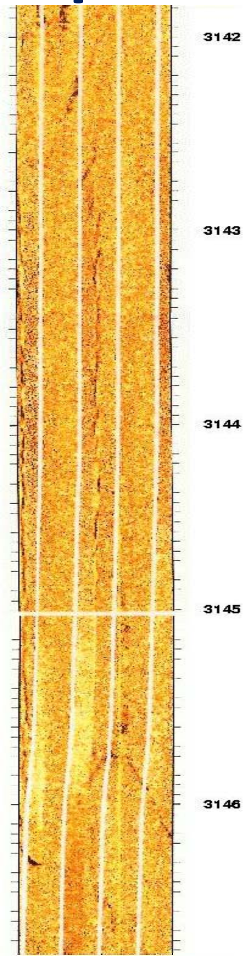

Caratérisation des variations d’orientation du nuage microsismique avec la profondeur

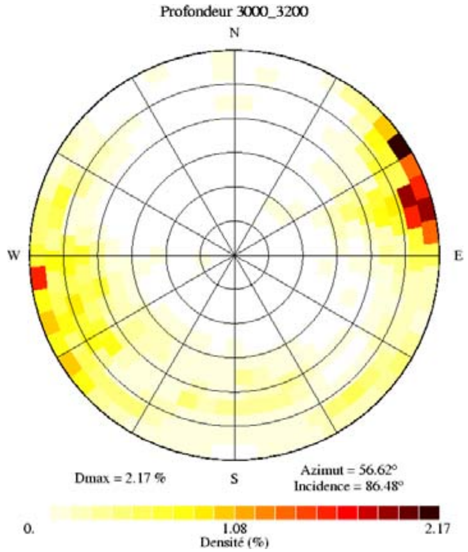

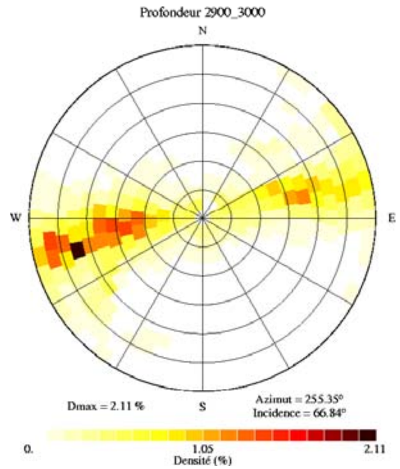

Depth interval (m)l	Mean azimuth	Mean dip	Number of events
2800 - 2900	N179°E	87°	329
2900 – 3000	N165°E	67°	402
3000 - 3200	N146°E	86°	416
1990 - 2200	N 147°E	87°	

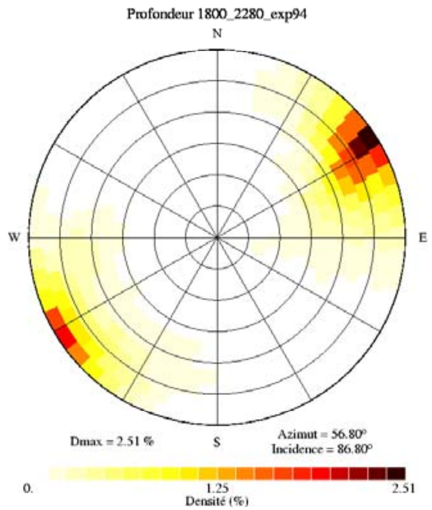

Variation des zones de d'injection en fonction de la pression d'injection

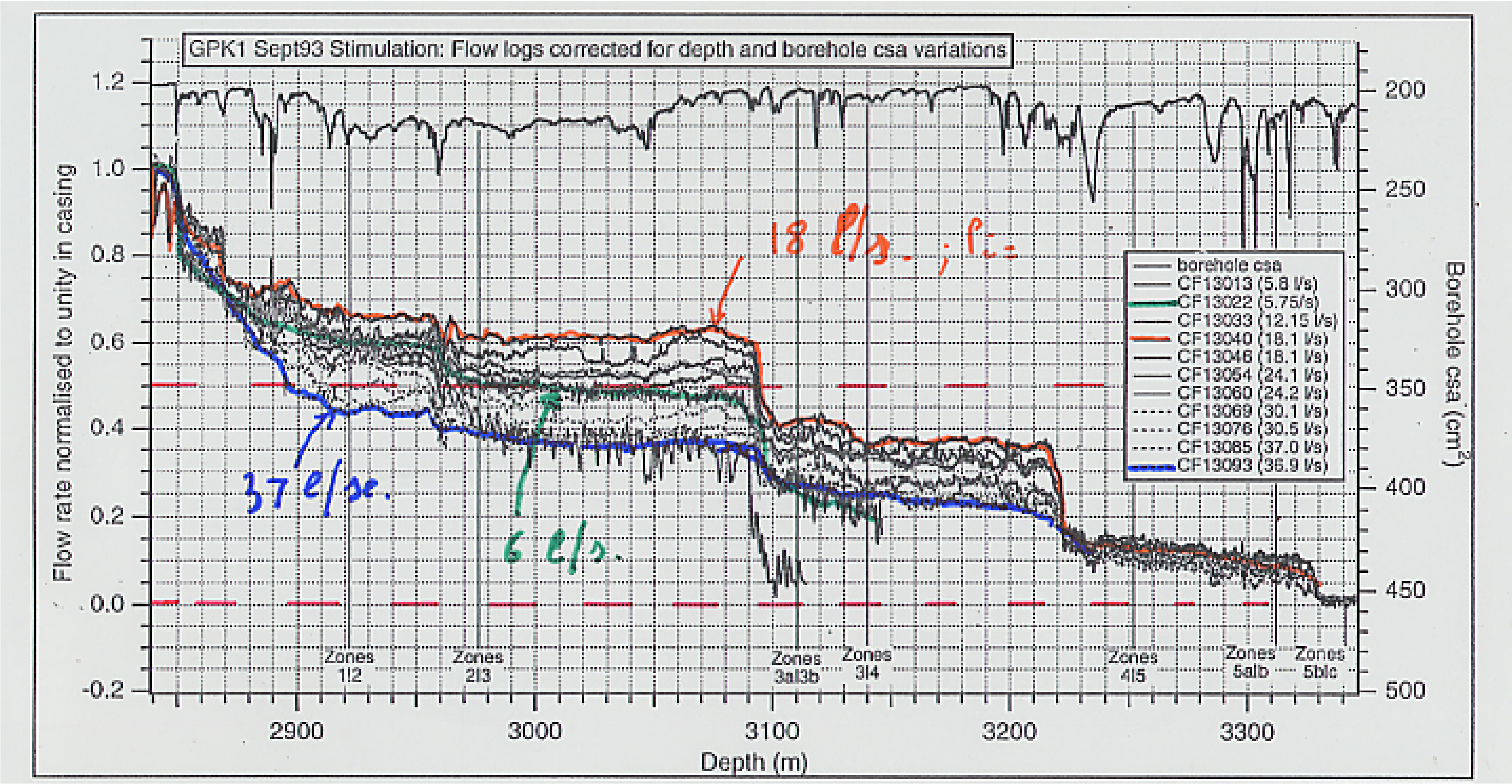

Le site de Soultz aujourd'hui

Present situation: four wells have been drilled.

All the wells have been stimulated by large progressive hydraulic injections at different depths and different periods to increase their connectivity.

Stimulated in 1993 at 2850-3600m

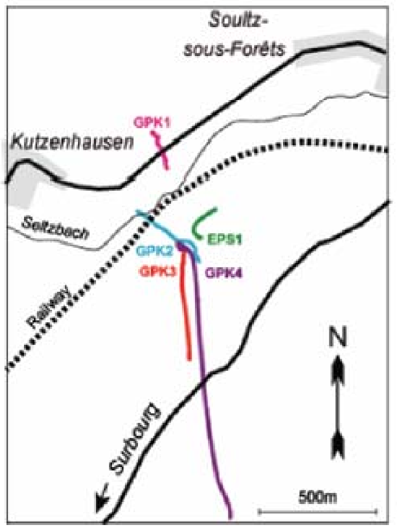

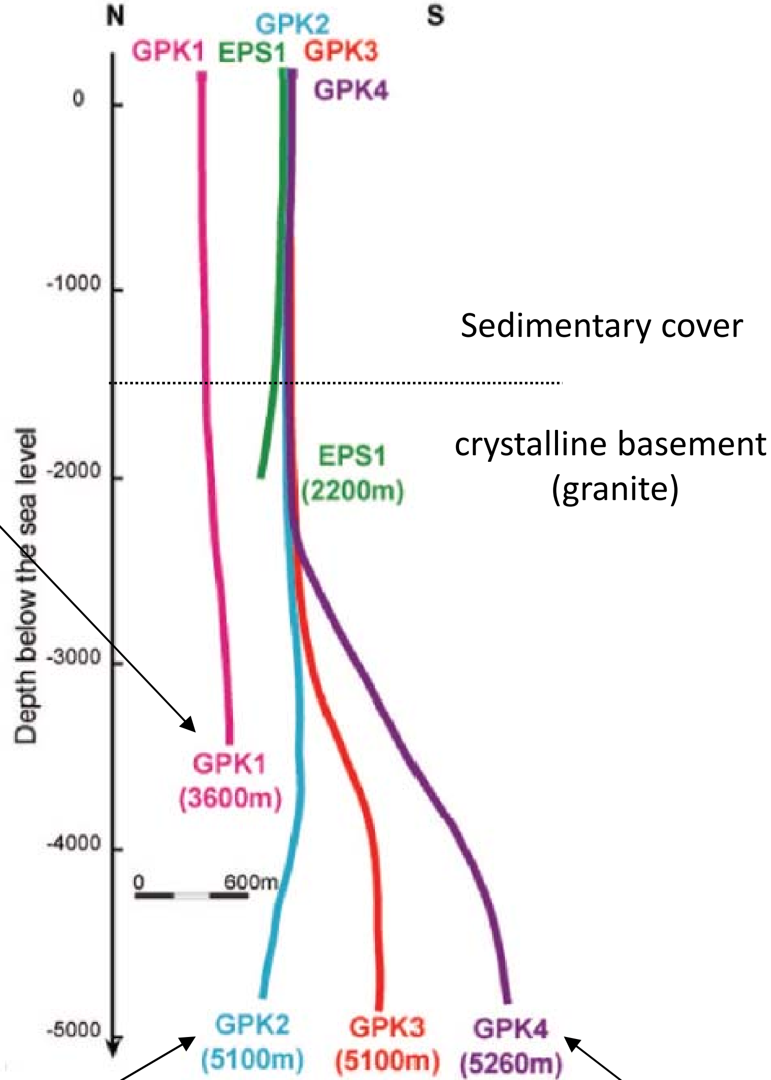

Stimulated in 1995 and 1996 at 3200-3800 m and in 2000 at 4400-5000 m

Stimulated in 2003 at 4487-5100 m

Stimulated in 2004 and 2005 at 4479-5000m

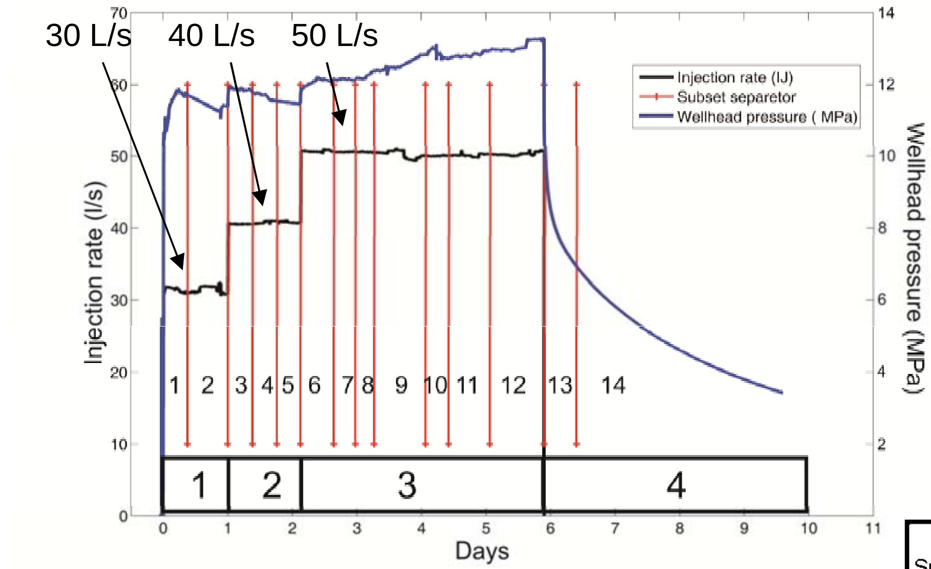

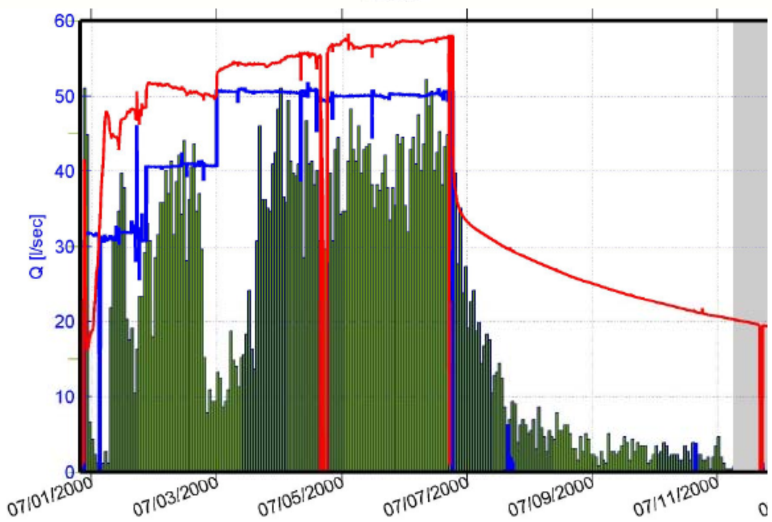

The whole period of the injection test has been divided into four main phases; 3 during the stimulation and 1 post-stimulation

Time domains seismic tomography with data sets adapted to the injection parameters. **(Calo' et al., JGI, 2011)**

We decided to apply the tomographic method to fourteen not-equally populated sets to better fit the sub set separation with the hydraulic parameters of the injected fluids (injection rate and wellhead pressure).

Data and subset selection

Subset	Time period renge	N. events	abs. P phases	abs. S phases	diff. P data	diff. S data
1	06/30 h 19:15	300	3131	1162	32839	9167
	07/01 h 03:40					
2	07/01 h 03:41	600	6443	1874	65316	15351
	07/01 h 18:39					
3	07/01 h 18:39	630	5807	2105	59163	17907
	07/02 h 03:50					
4	07/02 h 03:50	490	6807	1782	43582	14809
	07/02 h 12:57					
5	07/02 h 12:58	240	2246	674	23429	6324
	07/02 h 21:39					
6	07/02 h 21:46	490	4382	900	44049	6402
	07/03 h 10:04					
7	07/03 h 10:04	550	5836	2040	59341	17470
	07/03 h 18:06					
8	07/03 h 18:07	540	5745	2068	58460	17391
	07/04 h 10:25					
9	07/04 h 10:32	780	7192	2545	71515	22830
	07/04 h 20:11					
10	07/04 h 20:12	480	4493	1344	47121	12977
	07/05 h 04:45					
11	07/05 h 04:47	600	6701	2469	63488	20140
	07/05 h 20:06					
12	07/05 h 20:07	780	8659	3440	81361	20140
	07/06 h 16:10					
13	07/06 h 16:10	285	3213	1328	28826	11296
	07/07 h 04:18					
14	07/07 h 04:32	450	5098	1951	43835	13977
	07/11 h 00:55					

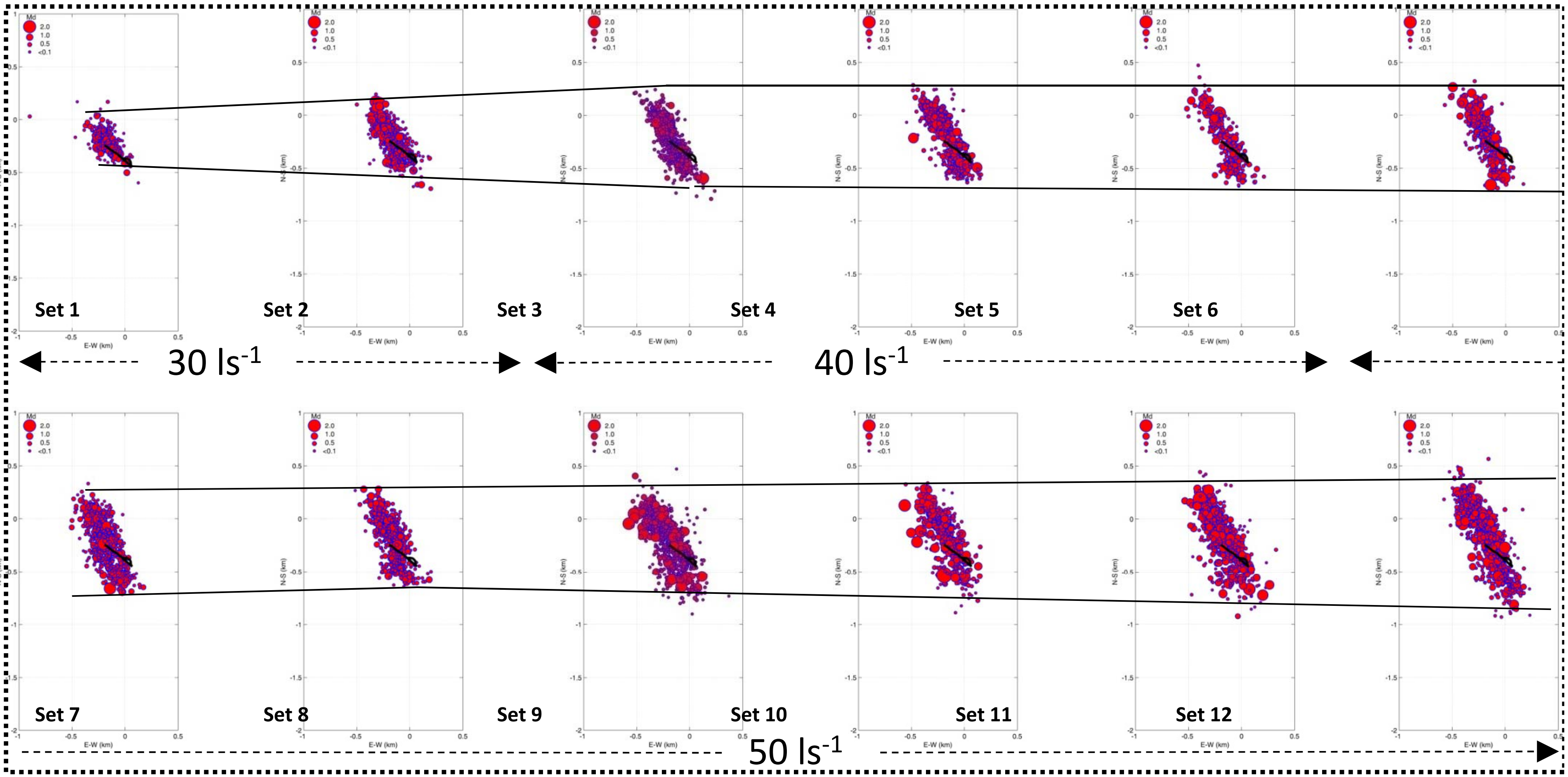

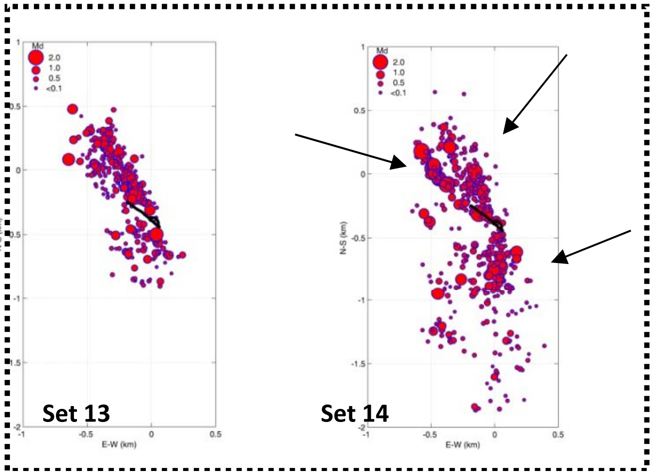

Seismicity re-located with the 3D velocity models.

No internal structure observed during the stimulation (sets 1-12). But the post-injection seismicity (sets 13 and 14) reveals oriented structures

Calò et al., JGI, 2011

Conclusion sur l'injection forcée

- On note quatre types de réponse selon l'amplitude de la pression d'injection:
  - Réponse élastique du système;
  - Circulation forcée dans réseau de fractures existant avec déstabilisation locale dans les plans préexistants quand $\tau = tg\phi (\sigma_n - P) + C$; ø et C angle de frottement et cohésion (=0?) de la fracture préexistante concernée.
  - Création d'une nouvelle zone de rupture en cisaillement

$\tau = tg\phi_0 (\sigma_n - P) + C_0$; ϕ_0 angle de frottement interne du matériau; orientation de la normale au plan de rupture à $(\pi/4 + \phi_0/2)$ de la direction de σ_{max}; C_0 cohésion de la roche saine;

  - Développement d'une fracture hydraulique si $P_{inj} \geq \sigma_{min}$ perpendiculaire à σ_{min} .

Le problème posé par l'exploitation des « gaz de schistes »